ARTICLES

nature photonics

Optical control of one and two hole spins in interacting quantum dots

Alex Greilich[1,2†], Samuel G. Carter[1], Danny Kim[1,3†], Allan S. Bracker[1] and Daniel Gammon[1*]

A single hole spin in a semiconductor quantum dot has emerged as a quantum bit that is potentially superior to an electron spin. A key feature of holes is that they have a greatly reduced hyperfine interaction with nuclear spins, which is one of the biggest difficulties in working with an electron spin. It is now essential to show that holes are viable for quantum information processing by demonstrating fast quantum gates and scalability. To this end, we have developed InAs/GaAs quantum dots coupled through coherent tunnelling and charged with controlled numbers of holes. We report fast, single-qubit gates using a sequence of short laser pulses. We then take the important next step towards scalability of quantum information by optically controlling two interacting hole spins in separate dots.

A semiconductor qubit offers powerful advantages for quantum information, including a scalable solid-state platform, integration with electronic or photonic circuits[1], ultrafast optical control[2–8] and relatively long lifetimes[9–11]. Until recently, most efforts in semiconductors made use of the spin of the electron as a qubit. However, a major difficulty when using electron spins is the strong hyperfine interaction, which couples the qubit to a bath of nuclear spins[12]. Random fluctuations of the nuclear spin polarization lead to electron spin dephasing. In the self-assembled InAs/GaAs quantum dots (QDs) discussed in this Article, the dephasing time $T_2^\star$ is typically 1–2 ns (refs 6,13), whereas in larger, electrically defined or interface fluctuation QDs, $T_2^\star$ is 5–10 ns (refs 2,14). This nuclear spin problem has motivated studies of hole spins, which have an order of magnitude weaker hyperfine interaction[15–19]. Early optical studies have been quite promising, having demonstrated long spin relaxation ($T_1 \approx 1$ ms)[9,10] and dephasing ($T_2^\star > 100$ ns)[11] times in InAs self-assembled QDs.

Although a QD hole can be treated as a pseudo-spin qubit and optically measured and controlled like an electron, in many ways its properties are unique and interesting. A hole is the absence of an electron in the otherwise full valence band states. In the p-type valence states, spin–orbit interaction is strong, which profoundly changes the nature of the hole spin and makes its properties sensitive to electric fields, strain and variations in the confinement potential[20]. In particular, anisotropy in the confinement potential in self-assembled QDs (stronger confinement along the growth direction than the transverse direction) gives significant anisotropy in the spin properties, such as the Zeeman interaction[21]. Similarly, the hyperfine interaction for a heavy hole is highly anisotropic, with an approximately Ising-like (AS_zI_z) form[15]. This is predicted to greatly reduce dephasing in a transverse magnetic field[16], even beyond the order-of-magnitude naively expected, which could explain the long dephasing time that has been reported[11].

Moreover, hole tunnelling between two such QDs exhibits new phenomena such as electric field resonances of the g-factor[22], which can be used to control the spin for quantum operations[23], and reversal of the bonding and anti-bonding states[24]. Remarkably, and in contrast to the other spin interactions, the exchange interaction between two hole spins in two QDs is predicted to be approximately isotropic or Heisenberg-like ($J\mathbf{S}_1 \cdot \mathbf{S}_2$)[25]. As a result, the two-spin states should separate into a singlet and a set of degenerate (or nearly degenerate) triplets, and ideas for optically controlling entanglement of two spins developed for two electrons can be brought over to two holes[8].

With these differences between the spin of an electron and hole in mind, quantum control demonstrations are now needed to establish the viability of the hole as a qubit. We take this step by demonstrating ultrafast optical control of hole spins in a system of coupled QDs for three different regimes: (i) an effectively isolated single hole spin, (ii) weakly interacting hole spins and (iii) strongly interacting hole spins. These results are quite promising for hole spin qubits and suggest future opportunities and challenges.
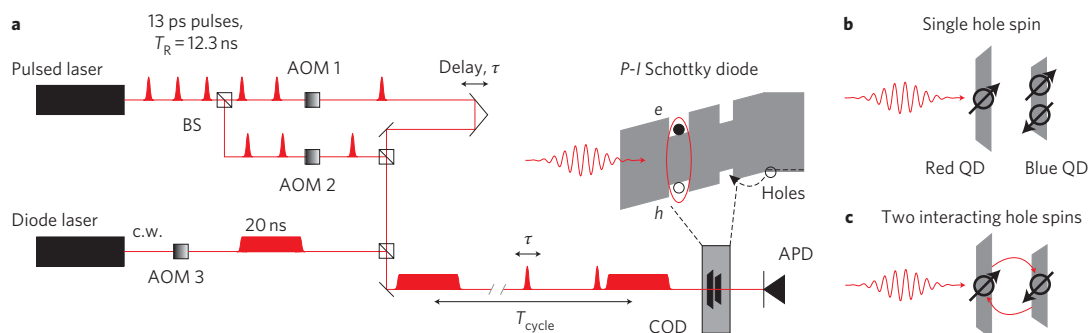
Holes in two tunnel-coupled QDs

We have developed a sample structure in which two vertically stacked QDs are grown within a p-type Schottky diode structure, and an applied voltage permits holes to be injected, one by one, into each of the QDs (Fig. 1). To characterize the system, optical absorption and emission are measured through continuous-wave (c.w.) resonant transmission and photoluminescence spectroscopy, respectively (Fig. 2). Both the configuration of holes and their corresponding optical transitions to excited states (X^+, X^{2+}, X^{3+}) are determined from the optical spectra. With increasing bias (left to right in Fig. 2a,b), the stable hole configurations in the two QDs go from (0,1) to (1,1) to (1,2) to (2,1), with vertical dashed lines in the figures separating the configurations. The numbers in parentheses correspond to the number of ground-state holes in each QD ('red', 'blue'). The optical transition for each of these charge configurations involves the excitation or recombination of an additional electron–hole pair in the red QD, as shown at the top of Fig. 2b. The blue transition is ~30 meV higher in energy. The optical resonance frequency shifts for each of the charge configurations because of differing Coulomb energies[26].

Anti-crossings of the spectral lines are a signature of coherent tunnelling between the two QDs[27–29]. In particular, an anti-crossing structure at –0.52 V to the left of the stable (1,1) voltage region corresponds to the exchange splitting between the singlet–triplet spin states[8]. This exchange splitting gradually decreases with increasing

---

[1]Naval Research Laboratory, Washington, District of Columbia 20375, USA, [2]University of Maryland, College Park, Maryland 20742, USA, [3]University of Michigan, Ann Arbor, Michigan 48109, USA; [†]Present address: Technische Universität Dortmund, 44221 Dortmund, Germany (A.G.); Harvard University, Cambridge, Massachusetts 02138, USA (D.K.). *e-mail: gammon@nrl.navy.mil

			Form Approved OMB No. 0704-0188

Report Documentation Page

Form Approved
OMB No. 0704-0188

Public reporting burden for the collection of information is estimated to average 1 hour per response, including the time for reviewing instructions, searching existing data sources, gathering and maintaining the data needed, and completing and reviewing the collection of information. Send comments regarding this burden estimate or any other aspect of this collection of information, including suggestions for reducing this burden, to Washington Headquarters Services, Directorate for Information Operations and Reports, 1215 Jefferson Davis Highway, Suite 1204, Arlington VA 22202-4302. Respondents should be aware that notwithstanding any other provision of law, no person shall be subject to a penalty for failing to comply with a collection of information if it does not display a currently valid OMB control number.

1. REPORT DATE **SEP 2011**	2. REPORT TYPE	3. DATES COVERED **00-00-2011 to 00-00-2011**
4. TITLE AND SUBTITLE **Optical control of one and two hole spins in interacting quantum dots**		5a. CONTRACT NUMBER
		5b. GRANT NUMBER
		5c. PROGRAM ELEMENT NUMBER
6. AUTHOR(S)		5d. PROJECT NUMBER
		5e. TASK NUMBER
		5f. WORK UNIT NUMBER
7. PERFORMING ORGANIZATION NAME(S) AND ADDRESS(ES) **Naval Research Laboratory,Washington,DC,20375**		8. PERFORMING ORGANIZATION REPORT NUMBER
9. SPONSORING/MONITORING AGENCY NAME(S) AND ADDRESS(ES)		10. SPONSOR/MONITOR'S ACRONYM(S)
		11. SPONSOR/MONITOR'S REPORT NUMBER(S)

12. DISTRIBUTION/AVAILABILITY STATEMENT
Approved for public release; distribution unlimited

13. SUPPLEMENTARY NOTES

14. ABSTRACT

15. SUBJECT TERMS

16. SECURITY CLASSIFICATION OF:			17. LIMITATION OF ABSTRACT	18. NUMBER OF PAGES	19a. NAME OF RESPONSIBLE PERSON
a. REPORT **unclassified**	b. ABSTRACT **unclassified**	c. THIS PAGE **unclassified**	**Same as Report (SAR)**	**7**	

Standard Form 298 (Rev. 8-98)
Prescribed by ANSI Std Z39-18

Figure 1 | Design of the experiment. a, Set-up configuration for Ramsey interference measurement, with a c.w. diode laser used to initialize and read out the spin polarization and a pulsed laser to induce spin rotation. T_R, repetition period of the laser; BS, non-polarizing beamsplitter; AOM, acousto-optic modulator; $T_{cycle} = 10T_R$; CQD, coupled quantum dots; APD, avalanche photodiode. **b**, CQD with a single hole spin in the red (lower transition energy) QD. Two spins in the blue QD inhibit any interaction with the red QD. Lasers are acting on the red QD only. **c**, CQD with one hole spin in each QD and interacting by a tunnelling-induced exchange interaction, J.
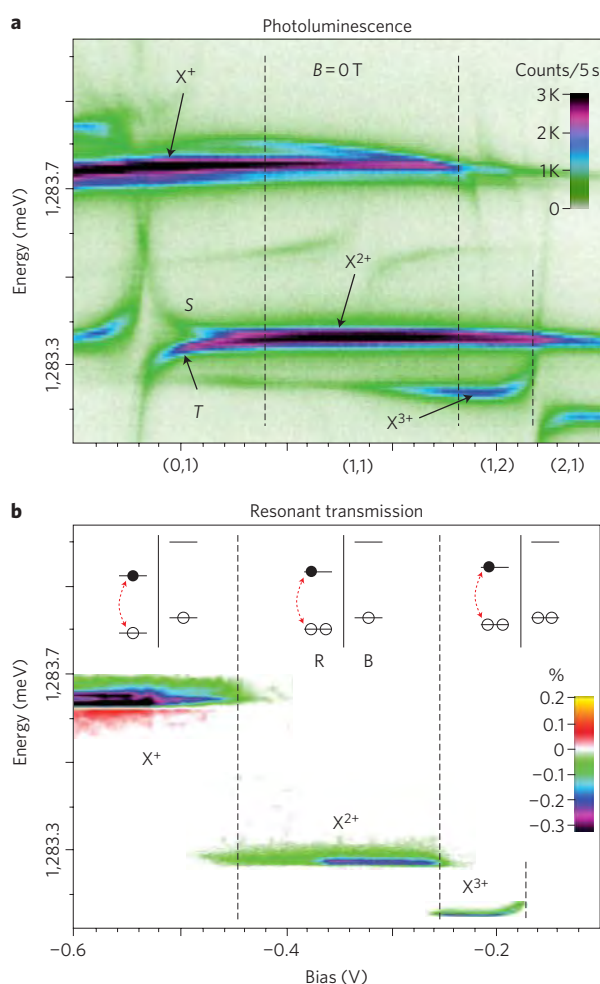
Figure 2 | Bias-dependent spectroscopy. a, Photoluminescence spectra of CQD at $B = 0$ T. Emission energy depends on the applied bias, showing different exciton charge complexes. The X-shaped pattern on the left gives a unique identification of the X^{2+} $\begin{pmatrix} \updownarrow & 0 \\ \Uparrow\Downarrow & \Updownarrow \end{pmatrix}$ charge configuration with triplets (T) and singlet (S) as the ground state. The S–T exchange splitting decreases for less negative bias and goes below the resolution of photoluminescence measurement (15 µeV). The X^{3+} (1,2) state is used for single hole spin control. **b**, Bias-dependent resonant laser absorption of the red dot. Dashed lines mark the stable regions of different charge configurations. R and B are the red and blue QDs, respectively.

bias, and in this sample is not resolved in the voltage region where the (1,1) configuration is stable. A model calculation (fit to the photoluminescence data) gives an exchange interaction of ~1 GHz, which is less than the optical linewidths (~2 GHz). We have also studied a second sample with a thinner tunnel barrier with a much larger exchange energy of ~20 GHz. The two-hole configuration (1,1) is of special interest because it permits us to demonstrate coherent optical control of two interacting hole spins.

Optical control of a single hole spin

We first demonstrated ultrafast optical control of a single hole spin, which has not previously been achieved. We can do this in the same QD structure simply by changing the voltage bias to the (1,2) configuration. By maintaining two spin-paired holes in the blue dot, the only degree of freedom is the single hole spin in the red dot (Fig. 1b). In a transverse magnetic field ($B_x = 6$ T), the two spin configurations of the (1,2) state and an optically excited state, X^{3+}, provide a three-level Λ system by which single spin initialization and rotation can be performed.

For our quantum control demonstration we applied a Ramsey interference technique to show control of the hole spin (Fig. 1a)[3,5,7,8]. A 20-ns-long pulse from a narrowband diode laser was used to prepare the spin of the hole by pumping one transition of the Λ-system (Fig. 3a)[10,30–33]. During this pulse, the hole spin was initialized to the $\Uparrow$ eigenstate of the system parallel to the magnetic field. This initial state is represented as the south pole of the Bloch sphere in Fig. 3b. Next, the Ramsey pulse sequence was applied. For this, we used two circularly polarized pulses, each of which rotates the spin about the optical axis k_z by $\pi/2$ (red arrows in Fig. 3b)[2–5]. Both pulses were 13 ps long (bandwidth, 150 µeV) and detuned 300 µeV below the low-energy transition to avoid real excitations. After the first pulse the hole spin is driven to the equator of the sphere where it starts to precess around the vertical axis, which is defined by the direction of the applied magnetic field B_x. After delay τ, the second pulse rotates the spin vector towards the north or south pole, depending on the phase, thus converting the phase into a population. This population was determined by measuring small changes in the transmission of the diode laser pulse. This initialization/rotation/measurement cycle was repeated with a period ten times that of the repetition period of the laser ($T_{cycle} = 10T_R = 123$ ns) and an averaged signal was plotted as Fig. 3c.

From the Ramsey fringe curve we can obtain the dephasing time of the single-hole spin. The hole spin coherence persists with little decay for the first 5 ns (the weak signal near zero delay will be discussed later). We extended the delay by one and then two laser repetition periods of 12.3 ns to measure the decay of the phase oscillations. Figure 3d shows the corresponding signal fitted to a
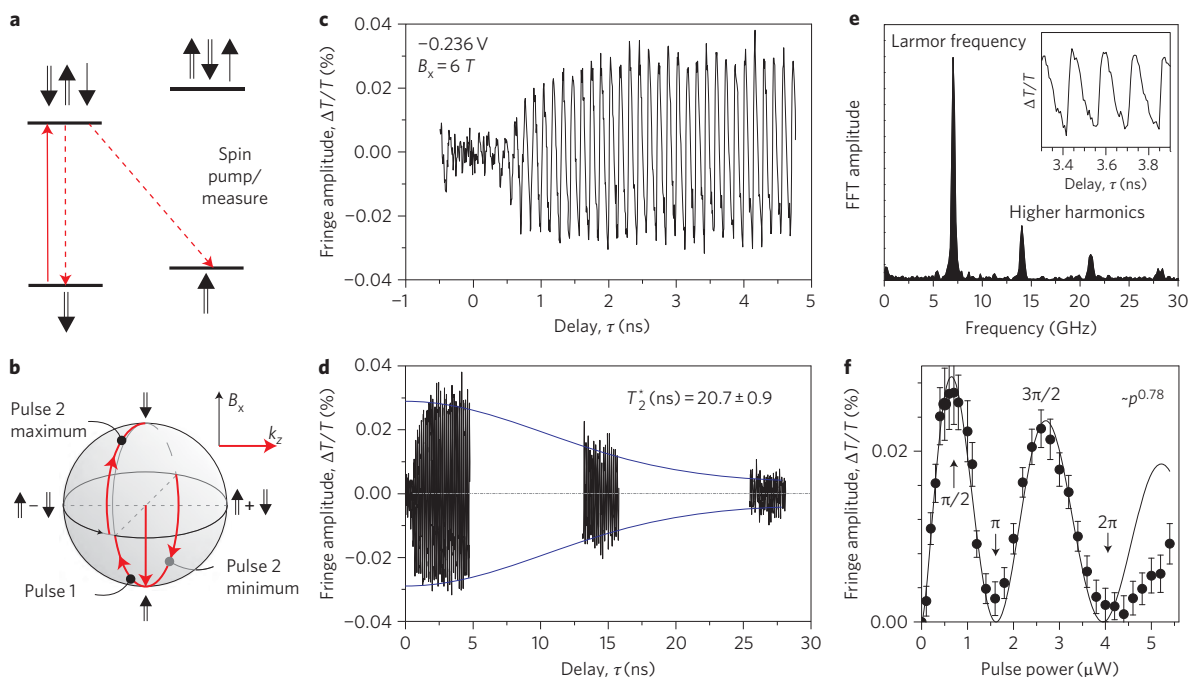
Figure 3 | Single hole spin control. a, Λ-level diagram for a single hole spin in transverse magnetic field. The red solid arrow shows the c.w. diode laser. Dashed lines are the recombination paths. **b**, Bloch sphere representation of the hole spin. The magnetic field rotates the spin around the vertical axis labelled B_x (see black arrow around equator), and the optical field rotates the spin around the optical axis labelled k_z (see red arrows moving up the sphere). Depending on the phase evolution, the second pulse brings the spin back to its initial state or to the opposite spin state. **c**, Ramsey fringe experiment with two $\pi/2$ pulses. **d**, As in **c**, but with extended delay. Blue envelope line is the fit with Gaussian decay constant T_2^*. **e**, Fourier transform of spectra in **c**. Inset: sawtooth form of the signal, which gives rise to the higher harmonics. **f**, Pulse power dependence. Black solid line is the fit using $\exp(-p/\tau) \sin(\omega p^x)^2$, with $x = 0.78$. Error bars are obtained from fits to the Ramsey fringes at each power and represent one standard error.

Gaussian envelope that decays with an inhomogeneous dephasing time $T_2^* = 20.7$ ns. This value is an order of magnitude larger than that measured for electrons in similar studies of self-assembled In(Ga)As QDs[6,13]. In these earlier studies, dephasing was limited by the interaction of the electron spin with the fluctuating nuclear environment. Although the hyperfine interaction may induce some dephasing here, we find that T_2^* is instead limited by electrical-noise-induced fluctuations in the hole g-factor. In other words, because the hole precession frequency varies with voltage, with a slope of ~10 MHz mV^{-1}, fluctuations in the electrical potential lead to fluctuations in the precession frequency. In this sample we have voltage fluctuations of a few millivolts (see Methods), which should give a T_2^* of tens of nanoseconds, which is consistent with the measured value. This result demonstrates that the hyperfine contribution to T_2^* is at least an order of magnitude weaker than for electrons. A previous experiment has reported a T_2^* greater than 100 ns, using frequency-domain measurements[11]. This longer time may indicate that electrical-noise-induced fluctuations of the g-factor were smaller in that sample, perhaps because there may be less impurity-induced electrical noise.

Although hyperfine interactions are not dominant in the dephasing of the hole spin, there is evidence that they are involved in its evolution. This is seen in the sawtooth form of the fringe pattern in Fig. 3c (see also Fig. 3e, inset). This behaviour was previously observed in the Ramsey fringes of an electron spin, and was explained by nuclear spin dragging[34]. The origin is likely the same here (see Methods). This effect is also seen through the Fourier transform of the signal (Fig. 3e). The main peak at 7 GHz corresponds to Larmor precession of the hole spin in the transverse magnetic field of $B_x = 6$ T, giving a hole g-factor in the red QD of 0.084. The higher harmonics are the result of the sawtooth form of the time-domain signal. Line following and hysteresis in the c.w.

transmission spectra are also observed here, an effect that has previously been shown to arise from feedback with the nuclear system in c.w. studies of electron systems[35,36]. We suspect that the small signal for short delays is due to these nuclear dragging effects, which can shift the transition out-of-resonance with the laser.

Full control of the hole spin, that is, rotation about an arbitrary axis by any angle, is achieved by a combination of optical pulse power, which rotates the spin up the Bloch sphere, and time delay, which allows precession around the sphere[3]. To demonstrate this, we measured the amplitude of the Ramsey fringes as a function of pulse power as displayed in Fig. 3f. The first maximum occurs for two $\pi/2$ pulses and the first minimum for two π pulses. These oscillations (essentially spin Rabi oscillations) confirm that this pulse sequence can optically rotate the hole spin to any point on the Bloch sphere and thus satisfy the requirements for qubit implementation. We find that the spin rotation angle has a sublinear dependence on power (~$p^{0.78}$). This behaviour is a result of insufficient pulse detuning for adiabatic elimination of the exciton state, as reported in previous studies of electron spin[3,8].

Optical control of two hole spins: weak interaction
For this experiment, the voltage bias on the sample was adjusted to give the stable two-hole configuration, (1,1), where the holes are in separate dots. Again, we directly control and measure the spin in the red QD with near-resonant optical pulses. As the exchange splitting is not larger than the optical transition linewidths in the stable region of this sample (Fig. 2), transitions in the red QD are not sensitive to the spin state in the blue QD. In this limit, we can draw the level diagram in Fig. 4d as two Λ-systems, differing only in the spin state of the blue QD. The initialization/measurement laser pumps two transitions (solid arrows) that are not resolved, initializing
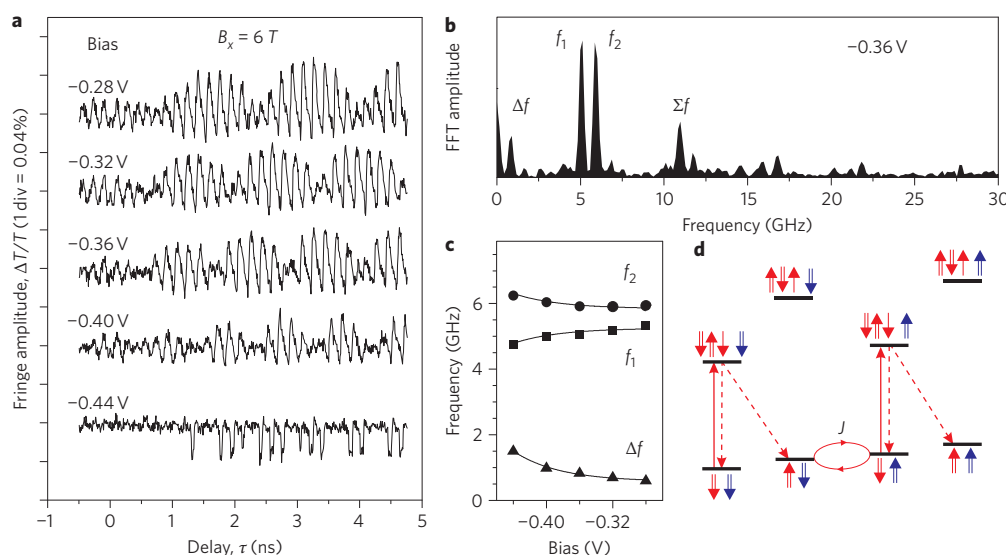
Figure 4 | Two weakly interacting hole spins. a, Ramsey fringe experiment for different biases corresponding to different exchange values. **b**, Fourier transform spectrum demonstrating two frequencies, f_1 and f_2, and their sum and difference frequencies caused by nonlinear effects. **c**, Bias dependence of f_1, f_2 and Δf from Fourier transforms. Lines are calculated using exchange splitting from the photoluminescence in Fig. 2a. **d**, Double Λ-level diagram for optical transitions of the red QD (red arrows) with exchange (J) with the blue QD. Blue dot (shown in blue) is not accessed optically.

into an incoherent mixture of $\Uparrow\Downarrow$ and $\Uparrow\Uparrow$. The short pulses also act on both Λ-systems, performing spin rotations on the red QD spin, regardless of the blue QD spin. The hole spin in the blue QD is not directly controlled, but it interacts with the spin in the red QD through the exchange interaction J. The resulting Ramsey fringe signal is shown in Fig. 4a. There is a clear beating in the data that depends on the voltage. In the Fourier transform it is seen that the peak at the Larmor spin resonance has split into two, with a splitting given by the exchange frequency (Fig. 4b). In addition, there are additional peaks at sums and differences of these primary resonance frequencies that come from nonlinearities arising from interactions with the nuclear spin, as in the single spin case.

We identify the beating in the Ramsey fringes as tunnelling-induced exchange between the QD spins, which is tuned with applied voltage. If the blue dot has spin up (down) the precession frequency of the red dot spin is shifted up (down) by $J/2$. Because the hole spin in the blue QD is not initialized up or down, averaging over these two possible initial conditions gives a beating at J. The voltage dependence of the beating frequency (Fig. 4c) is consistent with the exchange frequency deduced from the photoluminescence spectrum. In addition, with decreasing magnetic field we find that the Larmor frequency (average of f_1 and f_2) decreases but the beating frequency (difference between f_1 and f_2) does not, as expected. Finally we note that the measured $T_2^{\star}$ for the coupled hole spins (21 ns) is approximately the same as that for the single hole spin, again because of electric field fluctuations of the g-factor.

Optical control of two hole spins: strong interaction

With the first sample we are in a regime of small exchange coupling. With the second sample we increase the exchange interaction by an order of magnitude to provide distinct singlet and triplet lines in the stable region of the charging sequence. A laser field resonant with the red QD can then be used to initialize to the singlet state. Figure 5a presents a photoluminescence map of this sample at zero magnetic field. The two lower energy lines correspond to emission from the X^{2+} exciton states to the singlet and triplet spin states of the (1,1) charge configuration.

The level diagram for the (1,1) configuration is presented in Fig. 5b, in which the eigenstates are now written in the singlet–triplet basis. The singlet, $S = (|\Uparrow\Downarrow\rangle - |\Uparrow\Downarrow\rangle)/\sqrt{2}$, and $m_{\mathrm{s}} = 0$

triplet, $T_0 = (|\Uparrow\Downarrow\rangle + |\Uparrow\Downarrow\rangle)/\sqrt{2}$, are part of two lambda systems that differ in the helicity of their circular polarization selection rules. The other triplets, $T_+ = |\Uparrow\Downarrow\rangle$ and $T_- = |\Uparrow\Downarrow\rangle$ are nominally not connected to S and T_0 through optical transitions. However, we find that optical pumping can deplete the $T_\pm$ states, most likely due to hyperfine coupling of electron or hole spins that mixes the X^{2+} states or triplet states, respectively. With the laser resonant with the triplets, we can thus initialize the system into the singlet state, in which the hole spins are entangled[8].

Ramsey fringe experiments were performed in this system (shown in Fig. 5c) at a bias of –0.6 V and zero magnetic field. The optical pulses are short enough ($\sim$13 ps) compared to the exchange interaction that they still act as single qubit rotations on the red QD. On the S–T_0 Bloch sphere (see inset), the pulses rotate S towards T_0 (ref. 8). Initializing to the S state with a c.w. laser on the triplets, the first pulse rotates the Bloch vector to the equator, generating a superposition of S and T_0 that evolves in time. The Ramsey fringes observed here, in contrast to those presented previously in this Article, are not due to precession in an external magnetic field. Instead, they are entirely due to the interaction between hole spins.

The frequency of the Ramsey fringes is $\sim$20 GHz, consistent with the S–T splitting in Fig. 5a at this bias. However, there is a beating in the Ramsey fringes at a frequency of 1.9 GHz. We assert that this beating is due to a zero-field splitting between $T_\pm$ and T_0. One frequency is due to a S–T_0 superposition and one to a S–$T_\pm$ superposition. This splitting likely arises from an anisotropic contribution of $\sim$10% to the isotropic Heisenberg exchange. This anisotropic exchange is another manifestation of the stronger spin–orbit character of the holes. With this assumption we are able to model well the measured fringe pattern, as shown in Fig. 5c.

The fringe pattern decays significantly faster in this second sample ($T_2^{\star} < 600$ ps), again because of electrical noise. However, now it is because the exchange splitting is a strong function of voltage. The frequencies of the Ramsey fringes are plotted in Fig. 5d as a function of voltage, with the S–T splitting measured in transmission plotted for comparison. The large variation of the exchange frequency with bias (70 MHz mV^{-1} at –0.6 V) means the system is sensitive to electrical noise. Indeed, we find that $T_2^{\star}$ gets shorter at higher voltages as this slope increases, indicating that it plays a major role in dephasing. This dephasing could be
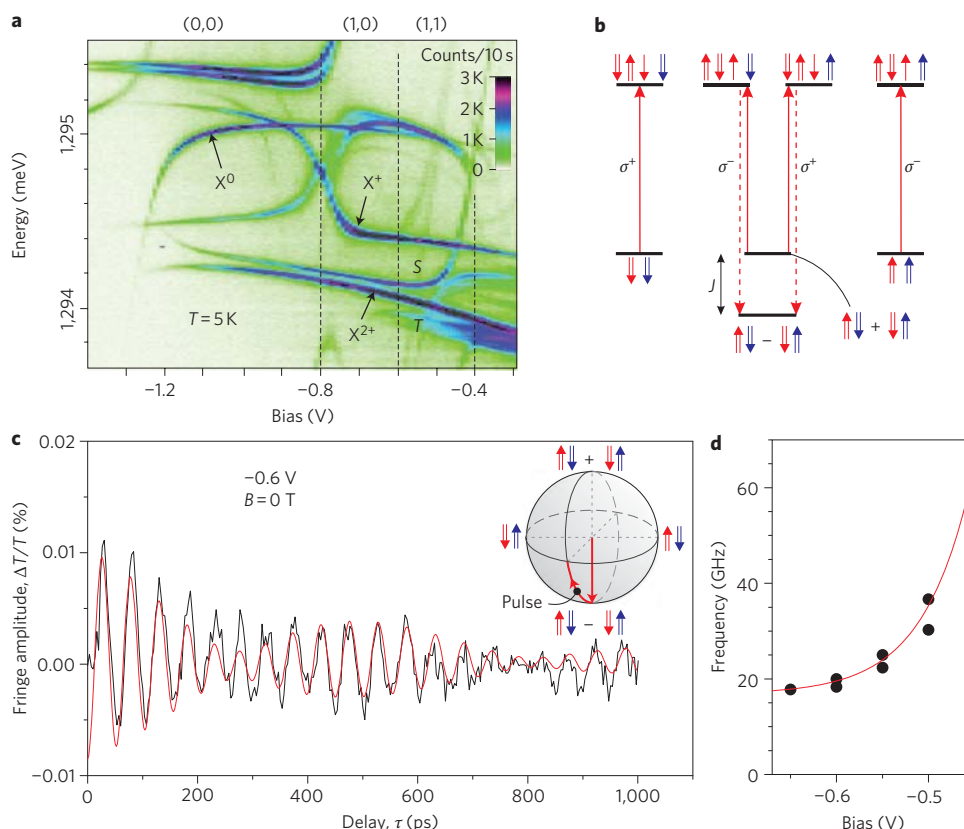
Figure 5 | Two strongly interacting hole spins. a, Photoluminescence spectra at $B = 0$ T. The X-shaped pattern corresponds to the X^+ charge configuration, with the hole moving between the two QDs. The two lower energy lines correspond to the triplets (T) and singlet (S) of the X^{2+} charge configuration with one hole in each QD. Dashed vertical lines mark the stable regions of different charge configurations. **b**, Level diagram for optical transitions of the red QD for an isotropic exchange interaction. Double (single) arrows represent hole (electron) spins. **c**, Ramsey fringes at -0.6 V. Black curve is experimental data, and the red curve is a model fit. The system is initialized into the singlet by optically pumping out of the triplets. The fast oscillations are between triplet and singlet states. The inset shows the singlet–triplet Bloch sphere. **d**, Fringe frequencies (solid circles, from the Ramsey data) and singlet–triplet splitting (red line, from transmission data) versus applied bias. The splitting seen in the fringe frequencies (but not resolved in the transmission data) corresponds to the slow beating seen in **c** and is discussed in the text.

minimized by optimizing the sample structure to shift the stability range of the (1,1) configuration to the minimum of the S–T splitting, where the slope is zero.

Discussion

We have presented fast, coherent rotations of a single hole spin, and also the first demonstration of two interacting hole spins in two QDs. The dephasing time of the hole was an order of magnitude longer than that reported for a single electron in a similar QD system with similar measurements[6,13]. Instead of being limited by the hyperfine interaction, the hole spin dephasing time is primarily determined by electrical-noise fluctuations that affect the spin through the spin–orbit interaction. We expect dramatic improvements in the dephasing time by reducing electrical-noise fluctuations or by engineering the system to be less sensitive. Also, because these environmental interactions typically evolve much more slowly than the hole spin system, spin echo techniques should lead to much longer lifetimes, as shown recently for electron spins[6]. In fact, preliminary spin echo measurements show significant enhancements in the dephasing time of the hole spin.

Controlling the interaction between spins is also essential, as it is the basis for two-qubit gates. We have succeeded in generating a tunable interaction between spins of tens of gigahertz, orders of magnitude higher than in any other system, while retaining single qubit control using short optical pulses. The interaction is also largely isotropic, and sensitivity to electric fields can clearly be

substantially improved. In the current systems the interaction between spins is tunable but always on, which may make it challenging to realize controllable interactions between many qubits. One advantage of hole spin qubits is that we can dramatically reduce the tunnelling interaction of holes in the ground state due to the large effective mass of holes[37]. The interaction can instead be produced in the excited states through electron tunnelling or exciton–exciton interactions, giving ultrafast optical pulse control of the interaction[38–40].

After submission of this Article, two other papers have appeared that describe optical coherent control of a single hole spin[41,42].

Methods

Sample structure. Two vertically stacked InAs dots were grown by molecular beam epitaxy on a p^+ GaAs substrate and embedded in a GaAs Schottky diode. A QD density of ~ 1 μm^{-2} was obtained with a gradient growth method. The two samples consisted of a p-type Be-doped buffer layer, a 25 nm GaAs spacer barrier, two InAs dot layers of 2.8 and 3.2 nm separated by a 4 nm or 6 nm GaAs tunnel barrier, and a 280 nm GaAs capping layer. The top dot was grown thicker than the bottom dot to give it the lower energy optical transition, so that only holes coherently tunnelled between the QDs[37]. The absorption linewidths in the samples were measured to increase with the slope of the Stark shift, which we attribute to electrical fluctuations that give rise to fluctuations in the transition energy. A voltage fluctuation of 4.3 mV was derived from the linear fit to the linewidth versus slope of the Stark shift for the X^{3+} transition.

Measurement techniques. The sample surfaces were covered with a 5 nm layer of titanium and a 120-nm-thick aluminium layer, which was patterned with 1 μm apertures such that single pairs of QDs could be measured. The sample was placed on piezo-stages in a helium flow cryostat at 5 K. A 0.68 NA aspheric lens was placed

in the cryostat to focus the laser on the aperture and also to collect the light for the photoluminescence measurements. Light transmitted through the aperture was focused onto an avalanche photodiode. The resonant transmission signal was probed by means of Stark-shift modulation spectroscopy using narrow-linewidth c.w. laser (nanoelectronvolt range) and lock-in techniques. The sample was modulated with a square-wave voltage at 10 kHz superimposed on the fixed d.c. voltage for phase-sensitive detection of the transmitted intensity. For the Ramsey fringe experiments, a Ti:sapphire laser was used with 13 ps pulses and a repetition period of 12.3 ns. Circular polarization of pulses was opposite to that of the c.w. probe and was rejected using a polarizer. Pulses were detuned below the low-energy exciton transition by 200–300 μeV.

Nuclear hysteresis effects. The sawtooth behaviour observed in the Ramsey fringes can be understood in essentially the same way as for the case of electron spins in ref. 34. The basic idea is that the rate of nuclear spin flips is proportional to the excitation probability by the initialization/measurement pulse, which depends on the precession phase at the second pulse. As in ref. 41, a random walk of the nuclear polarization changes the precession frequency ω until the commensurate condition, $\omega\tau = 2\pi n$, is satisfied, at which no excitation or nuclear spin flips occur. As the pulse delay is slowly varied, the nuclear polarization adjusts to continue satisfying this condition, but jumps when it pushes the exciton transition out of resonance with the laser. This gives rise to the nonlinear sawtooth behaviour observed. We also suspect that the small signal for small delays is due to the fact that the nuclear polarization required to satisfy the commensurate condition is much larger for small τ, which tends to shift the transition out-of-resonance with the laser.

Interacting spin states. For the (1,1) hole configuration the ground-state spin eigenstates at zero magnetic field are the singlet, $S = (\Uparrow\Downarrow - \Downarrow\Uparrow)/\sqrt{2}$, and three triplets, $T_0=(\Uparrow\Downarrow + \Downarrow\Uparrow)/\sqrt{2}$, $T_- = \Downarrow\Downarrow$, and $T_+ = \Uparrow\Uparrow$. At high magnetic fields we expect a mixing of S and T_0 due to a difference in g-factors, Δg, between the red and blue QDs. The g-factor is sensitive to valence band mixing, which can vary from dot to dot and with orbital wavefunction changes. A significant difference of $\Delta g/g =$ 42% has been measured in the Faraday field geometry for the 6 nm barrier sample, and we expect a similar relative difference in the Voigt geometry. For $\Delta g\mu B \gg J$, the states and T_0 are mixed to give eigenstates of $\Uparrow\Downarrow + \delta\Downarrow\Uparrow$ and $\Uparrow\Downarrow - \delta\Downarrow\Uparrow$, where $2\delta = J/\Delta g\mu B \approx 0.4$. This limit is reasonable for the weakly interacting 6 nm barrier sample, and we can represent the ground states and exciton states as shown in Fig. 4d, where δ terms have been omitted for simplicity. We also note that the red dot precession frequency changes between the (1,2) and (1,1) configurations, going from 7 GHz to 5.5 GHz (average of the two frequencies, f_1 and f_2). This change is presumably due to a change in the orbital wavefunction in the red dot as the number of holes in the blue dot changes from two to one.

In the strongly interacting 4 nm barrier sample, the singlet–triplet states should be good eigenstates, because the exchange interaction is large and experiments are performed at zero magnetic field. The beating in the Ramsey fringes can be explained by anisotropy in the exchange interaction. For a Hamiltonian $H = J\mathbf{S}^R \cdot \mathbf{S}^B + 2J'S_Z^R S_Z^B$, the isotropic J term gives rise to the singlet–triplet splitting, and the J' term splits T_0 away from T_+ and T_- by J'. (S_z^R and S_z^B are spin operators for the red and blue QDs, respectively, with eigenvalues $\pm 1/2$.) The anisotropy axis, z in this Hamiltonian, determines the basis of the eigenstates. Our model of the Ramsey fringes gives a beating only when the anisotropy axis is between the growth direction and the plane of the QD. In this basis, the optical pulse rotates the S state to a superposition of all four basis states, giving rise to the different frequencies observed. The selection rules in Fig. 5b will also be modified in this basis, allowing diagonal transitions. The anisotropy and its orientation likely arise from the spin–orbit interaction combined with structural asymmetry, such as a relative lateral displacement of the two QDs[42].

Fidelity estimates. At $B = 0$ T no spin pumping was observed in the 6 nm barrier quantum dot sample. With higher magnetic fields the pumping was recovered, reaching the initialization fidelity of 91% at $B_x = 6$ T as estimated from the bleaching of the higher energy transition in the single-laser differential transmission. To calculate this we compared the bleached signal level with the signal, where pumping is suppressed by a single detuned π-pulse. The fidelity was then $F_{pump} = 1 - \alpha/\alpha_0$ = 0.91, where α is the signal level at 6 T and α_0 is the signal level with the π-pulse. We estimated the fidelity of single-qubit gates using data from Fig. 3f, which plots the Ramsey fringe amplitude as a function of pulse power. The oscillations show decay that we attribute to pulse-induced decoherence. From the fit to a decaying sine, we determined the expected amplitude for two π/2-pulses with no dephasing, A_{fit}, and compared this with the maximum signal at 0.66 μW, A_{meas}. If each pulse reduces the Bloch vector by a factor D, then $D^2 = A_{meas}/A_{fit} = 0.96$, giving a gate fidelity of $F = (1 + D)/2 = 0.99$ (ref. 3).

References

1. Englund, D., Faraon, A., Zhang, B., Yamamoto, Y. & Vuckovic, J. Generation and transfer of single photons on a photonic chip. *Opt. Express* **15**, 5550–5558 (2007).

2. Berezovsky, J., Mikkelson, M. H., Stoltz, N. G., Coldren, L. A. & Awschalom, D. D. Picosecond coherent optical manipulation of a single electron spin in a quantum dot. *Science* **320**, 349–352 (2008).

3. Press, D., Ladd, T. D., Zhang, B. & Yamamoto, Y. Complete quantum control of a single quantum dot spin using ultrafast optical pulses. *Nature* **456**, 218–221 (2008).

4. Greilich, A. *et al*. Ultrafast optical rotations of electron spins in quantum dots. *Nature Phys.* **5**, 262–266 (2009).

5. Kim, E. D. *et al*. Fast spin rotations by optically controlled geometric phases in a charge-tunable InAs quantum dot. *Phys. Rev. Lett.* **104**, 167401 (2010).

6. Press, D. *et al*. Ultrafast optical spin echo in a single quantum dot. *Nature Photon.* **4**, 367–370 (2010).

7. de Vasconcellos, S. M., Gordon, S., Bichler, M., Meier, T. & Zrenner, A. Coherent control of a single exciton qubit. *Nature Photon.* **4**, 545–548 (2010).

8. Kim, D., Carter, S. G., Greilich, A., Bracker, A. S. & Gammon, D. Ultrafast optical control of entanglement between two quantum-dot spins. *Nature Phys.* **7**, 223–229 (2011).

9. Heiss, D. *et al*. Observation of extremely slow hole spin relaxation in self-assembled quantum dots. *Phys. Rev. B* **76**, 241306(R) (2007).

10. Gerardot, B. D. *et al*. Optical pumping of a single hole spin in a quantum dot. *Nature* **451**, 441–444 (2008).

11. Brunner, D. *et al*. A coherent single-hole spin in a semiconductor. *Science* **325**, 70–72 (2009).

12. Merkulov, I. A., Efros, A. L. & Rosen, M. Electron spin relaxation by nuclei in semiconductor quantum dots. *Phys. Rev. B* **65**, 205309 (2002).

13. Greilich, A. *et al*. Mode locking of electron spin coherences in singly charged quantum dots. *Science* **313**, 341–345 (2006).

14. Petta, J. R. *et al*. Coherent manipulation of coupled electron spins in semiconductor quantum dots. *Science* **309**, 2180–2184 (2005).

15. Fischer, J., Coish, W. A., Bulaev, D. V. & Loss, D. Spin decoherence of a heavy hole coupled to nuclear spins in a quantum dot. *Phys. Rev. B* **78**, 155329 (2008).

16. Fischer, J. & Loss, D. Hybridization and spin decoherence in heavy-hole quantum dots. *Phys. Rev. Lett.* **105**, 266603 (2010).

17. Eble, B. *et al*. Hole–nuclear spin interaction in quantum dots. *Phys. Rev. Lett.* **102**, 146601 (2009).

18. Fallahi, P., Yilmaz, S. T. & Imamoglu, A. Measurement of a heavy-hole hyperfine interaction in InGaAs quantum dots using resonance fluorescence. *Phys. Rev. Lett.* **105**, 257402 (2010).

19. Chekhovich, E. A., Krysa, A. B., Skolnick, M. S. & Tartakovskii, A. I. Direct measurement of the hole–nuclear spin interaction in single InP/GaInP quantum dots using photoluminescence spectroscopy. *Phys. Rev. Lett.* **106**, 027402 (2011).

20. Winkler, R. *Spin–Orbit Coupling Effects in Two-Dimensional Electron and Hole Systems* (Springer-Verlag, 2003).

21. Bayer, M. *et al*. Fine structure of neutral and charged excitons in self-assembled In(Ga)As/(Al)GaAs quantum dots. *Phys. Rev. B* **65**, 195315 (2002).

22. Doty, M. F. *et al*. Electrically tunable g factors in quantum dot molecular spin states. *Phys. Rev. Lett.* **97**, 197202 (2006).

23. Andlauer, T. & Vogl, P. Electrically controllable g tensors in quantum dot molecules. *Phys. Rev. B* **79**, 045307 (2009).

24. Doty, M. F. *et al*. Antibonding ground states in InAs quantum-dot molecules. *Phys. Rev. Lett.* **102**, 047401 (2009).

25. Kavokin, K. Symmetry of anisotropic exchange interactions in semiconductor nanostructures. *Phys. Rev. B* **69**, 075302 (2004).

26. Scheibner, M., Bracker, A. S., Kim, D. & Gammon, D. Essential concepts in the optical properties of quantum dot molecules. *Solid State Commun.* **149**, 1427–1435 (2009).

27. Stinaff, E. A. *et al*. Optical signatures of coupled quantum dots. *Science* **311**, 636–639 (2006).

28. Krenner, H. J. *et al*. Optically probing spin and charge interactions in a tunable artificial molecule. *Phys. Rev. Lett.* **97**, 076403 (2006).

29. Doty, M. F. *et al*. Optical spectra of doubly charged quantum dot molecules in electric and magnetic fields. *Phys. Rev. B* **78**, 115316 (2008).

30. Atature, M. *et al*. Quantum-dot spin-state preparation with near-unity fidelity. *Science* **312**, 551–553 (2006).

31. Xu, X. *et al*. Fast spin state initialization in a singly charged InAs–GaAs quantum dot by optical cooling. *Phys. Rev. Lett.* **99**, 097401 (2007).

32. Kim, D. *et al*. Optical spin initialization and nondestructive measurement in a quantum dot molecule. *Phys. Rev. Lett.* **101**, 236804 (2008).

33. Vamivakas, A. N. *et al*. Observation of spin-dependent quantum jumps via quantum dot resonance fluorescence. *Nature* **467**, 297–300 (2010).

34. Ladd, T. D. *et al*. Pulsed nuclear pumping and spin diffusion in a single charged quantum dot. *Phys. Rev. Lett.* **105**, 107401 (2010).

35. Xu, X. *et al*. Optically controlled locking of the nuclear field via coherent dark-state spectroscopy. *Nature* **459**, 1105–1109 (2009).

36. Latta, C. *et al*. Confluence of resonant laser excitation and bidirectional quantum-dot nuclear-spin polarization. *Nature Phys.* **5**, 758–763 (2009).

37. Bracker, A. S. *et al*. Engineering electron and hole tunneling with asymmetric InAs quantum dot molecules. *Appl. Phys. Lett.* **89,** 233110 (2006).
38. Calarco, T., Datta, A., Fedichev, P., Pazy, E. & Zoller, P. Spin-based all-optical quantum computation with quantum dots: understanding and suppressing decoherence. *Phys. Rev. A* **68,** 012310 (2003).
39. Emary, C. & Sham, L. J. Optically controlled logic gates for two spin qubits in vertically coupled quantum dots. *Phys. Rev. B* **75,** 125317 (2007).
40. Economou, S. E. & Reinecke, T. L. Optically induced spin gates in coupled quantum dots using the electron–hole exchange interaction. *Phys. Rev. B* **78,** 115306 (2008).
41. De Greve, K. *et al*. Ultrafast coherent control and suppressed nuclear feedback of a single quantum dot hole qubit. *Nature Phys*. http://dx.doi.org/10.1038/nphys2078 (2011)
42. Godden, T. M. *et al*. Coherent optical control of the spin of a single hole in a quantum dot. Preprint at arXiv:1106.6282.
43. Greilich, A. *et al*. Nuclei-induced frequency focusing of electron spin coherence. *Science* **317,** 1896–1899 (2007).
44. Doty, M. F. *et al*. Hole–spin mixing in InAs quantum dot molecules. *Phys. Rev. B* **81,** 035308 (2010).

Author contributions

All authors were involved in the conception of the work and in writing the manuscript. A.S.B. grew and processed the samples. A.G., S.G.C. and D.K. performed the optical measurements. A.G., S.G.C. and D.G. performed data analysis and modelling.

Additional information

The authors declare no competing financial interests. Reprints and permission information is available online at http://www.nature.com/reprints. Correspondence and requests for materials should be addressed to D.G.